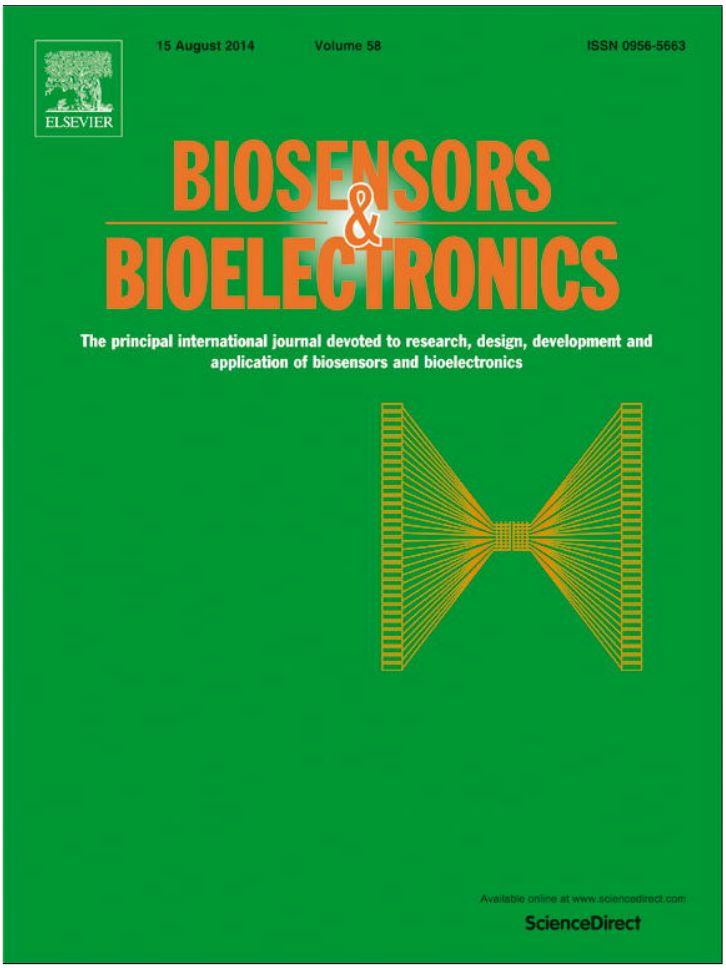

Biosensors and Bioelectronics 58 (2014) 165–171

Contents lists available at ScienceDirect

Biosensors and Bioelectronics

journal homepage: www.elsevier.com/locate/bios

Structure-selective hot-spot Raman enhancement for direct identification and detection of trace penicilloic acid allergen in penicillin

Liying Zhang [a], Yang Jin [a], Hui Mao [a], Lei Zheng [a], Jiawei Zhao [a], Yan Peng [a], Shuhu Du [a,*], Zhongping Zhang [b,**]

[a] School of Pharmacy, Nanjing Medical University, Nanjing, Jiangsu 211166, China
[b] Institute of Intelligent Machines, Chinese Academy of Sciences, Hefei, Anhui 230031, China

ARTICLE INFO

Article history:
Received 11 November 2013
Received in revised form
14 February 2014
Accepted 19 February 2014
Available online 2 March 2014

Keywords:
Core–shell nanoparticles
Sensor
SERS
Hot-spot
Penicilloic acid
Penicillin

ABSTRACT

Trace penicilloic acid allergen frequently leads to various fatal immune responses to many patients, but it is still a challenge to directly discriminate and detect its residue in penicillin by a chemosensing way. Here, we report that silver-coated gold nanoparticles (Au@Ag NPs) exhibit a structure-selective hot-spot Raman enhancement capability for direct identification and detection of trace penicilloic acid in penicillin. It has been demonstrated that penicilloic acid can very easily link Au@Ag NPs together by its two carboxyl groups, locating itself spontaneously at the interparticle of Au@Ag NPs to form strong Raman hot-spot. At the critical concentration inducing the nanoparticle aggregation, Raman-enhanced effect of penicilloic acid is ~60,000 folds higher than that of penicillin. In particular, the selective Raman enhancement to the two carboxyl groups makes the peak of carboxyl group at C_6 of penicilloic acid appear as a new Raman signal due to the opening of β-lactam ring of penicillin. The surface-enhanced Raman scattering (SERS) nanoparticle sensor reaches a sensitive limit lower than the prescribed 1.0‰ penicilloic acid residue in penicillin. The novel strategy to examine allergen is more rapid, convenient and inexpensive than the conventional separation-based assay methods.

1. Introduction

Penicillin has been one of the most widely used and highly-efficient antibacterial drugs for the clinical treatments of various infectious diseases, and saves a large number of lives of human as well as animals. However, allergic test is a necessary procedure before its use because the allergic responses for some patients are very serious and even fatal, for example, urticarial lesion, hypotension and anaphylactic shock (Mendelson et al., 1984; Pichichero, 2005; Sogn, 1984; Torres et al., 1999). It has now been clarified that penicilloic acid (PA) as the by-product in the synthesis of penicillin or the degradation product of penicillin in storage through the opening of β-lactam ring of penicillin is a major allergen causing the fatal immune responses by covalent conjugation with ε-amino groups of lysine residues of immunological proteins through penicilloyl groups (Batchelor et al., 1965, 1967; Blanca et al., 2001; Levine and Ovary, 1961; Smith and Marshall, 1971; Weltzien and Padovan, 1998). In general, the residual amount of PA less than 1.0% (w/w) in penicillin can significantly reduce the occurrence of allergic reactions. Therefore, the identification and measurement of trace PA residue in penicillin are important for the prevention of allergic reactions. Up to date, some detection methods for the screening of PA in penicillin have been reported, for example, colorimetric method (Pan, 1954), nuclear magnetic resonance (Degelaen et al., 1979), liquid chromatography–electrospray ionization mass spectrometry (Li et al., 2008) and enzyme-linked immunosorbent assay (Zhang et al., 2010). Due to the structural similarity to penicillin and the very trace amount in penicillin, the identification of PA usually requires the sophisticated sampling, beforehand separation/extraction and pre-concentration procedures in these above techniques, which are highly expensive or time-consuming and cause environmental problems. The method for the direct identification and detection of trace PA residue in penicillin has been a challenge.

With the integration of high sensitivity, unique spectroscopic fingerprints and nondestructive data acquisition, surface-enhanced Raman scattering (SERS) technique has become one of the most widely pursued spectroscopic tools for the identification and detection of chemical and biological species (Abbas et al., 2013; Qian and Nie, 2008; Smith, 2008). Theory of SERS is now largely established, in which most of the spectroscopic enhancement is attributed to the concentration of the electromagnetic (EM) optical fields near gold (Au)

* Corresponding author. Tel.: +86 25 86868476.
** Corresponding author. Tel.: +86 551 5591165.
E-mail addresses: shuhudu@njmu.edu.cn (S. Du), zpzhang@iim.ac.cn (Z. Zhang).

http://dx.doi.org/10.1016/j.bios.2014.02.052
0956-5663

or silver (Ag) nanoparticles (Jeanmaire and Van Duyne, 1977). The amplification of Raman signals can lead to a 10^6–10^{15} enhancement depending on the strength of EM experienced by the molecules at the surface of various metal nanostructures (Nie and Emory, 1997; Pieczonka and Aroca, 2008). Recently, various Ag and Au nanoparticle colloids have been widely investigated to develop highly SERS-active substrates (Brus, 2008; Camden et al., 2008a; Li et al., 2013; Wu et al., 2012). In particular, the core–shell Au@Ag nanoparticles exhibit stronger Raman enhancement than pure Au or Ag NPs owing to the wide and strong plasmonic resonance absorption, and can be used as stand-alone-particle Raman amplifiers, as reported in our previous work (Liu et al., 2012). On the other hand, the highest Raman enhancement usually occurs at the interparticle "hot-spot" in which the electromagnetic optical fields are highly concentrated (Camden et al., 2008b; Pieczonka and Aroca, 2008; Qian and Nie, 2008). It is thus expected that the ultrahigh hot-spot enhancement of Au@Ag interparticles can provide a direct spectroscopic identification of trace analytes in a structure-like matrix substance.

Here, we report the direct identification and detection of trace PA residue from penicillin using a SERS nanoparticle sensor. The interparticle hot-spot of Au@Ag NPs can be induced by PA linkage to Au@Ag NPs through the surface complexing interaction of two carboxyl groups of PA. In the presence of a large amount of penicillin, the hot-spot can selectively enhance the Raman signals of PA, and result in the characteristic Raman fingerprint of PA different from that of penicillin. The rapid, in situ assay of trace PA residue in penicillin has been thus achieved with the excellent sensitivity, selectivity and good repeatability.

2. Experimental section

2.1. Reagents and materials

Sodium citrate ($Na_3C_6H_5O_7 \cdot 2H_2O$, 99.8%), chloroauric acid ($HAuCl_4 \cdot 4H_2O$, 99.9%), silver nitrate ($AgNO_3$, 99%), and ascorbic acid (99%) were purchased from Sinopharm Chemical Reagent Co., Ltd. (Shanghai, China). Benzylpenicillin sodium was obtained from the North China Pharmaceutical Group Corporation (Shijiazhuang, China). All of these reagents were used without further treatment. Ultrapure water (18.2 MΩ cm) was produced using a Millipore water purification system (Milford, MA, USA).

2.2. Synthesis of Au@Ag NPs

The Au@Ag NPs were prepared using a two-step reduction method including the synthesis of Au cores and the subsequent growth of Ag shells, as described in our previous work (Du et al., 2013). The final concentration of Au@Ag NPs was estimated to be ~1.6 nM. See the details of synthesis in Supporting information.

2.3. Preparation and purification of PA

PA was prepared by alkaline hydrolysis of penicillin (Ghebre-Sellassie et al., 1984). Typically, 3.73 g of benzylpenicillin sodium was dissolved in 100 mL of 0.2 M NaOH at room temperature. The mixture was continuously stirred using a magnetic stirrer, and the pH remained greater than 12 in the reaction process. After 90 min, the pH was adjusted to 8.7 by the addition of 1.0 M HCl, and then the mixture was lyophilized. The resultant product was dissolved in anhydrous ethanol. PA crystallized from the ethanol solution at 4 °C after moderate acetonitrile was slowly added into above solution under rapid stirring. The characterization of mass spectroscopy (MS) gave *m/z*: 353.1 $[M+1]^+$ for the final product (the inset of Fig. S3B), which was completely consistent with the molecular weight of PA.

2.4. Theoretical calculations

The conformation search of PA molecule and the molecular vibrational bands of the investigated compounds were performed with a Gaussian 09 program package. See Supporting information for details.

2.5. Measurements of SERS of PA and penicillin

In brief, 0.5 M PA solution was prepared and diluted with ultrapure water to the predetermined concentrations. Then, 10 μL of the analyte solution was added into 90 μL of Au@Ag NPs colloids in a 1.5 mL centrifuge tube, followed by shaking for 1 min. The mixture was first sucked into a capillary glass tube, which was then fixed onto a glass slide. The Raman spectra were recorded using a 532-nm laser with 10 mW power and 10 × objective. The collecting time was 10 s with 5 rounds of accumulations and the pinhole aperture was 25 μm. Penicillin was also tested using the same method.

2.6. SERS detection of PA in spiked penicillin

Briefly, PA with different amounts was first spiked into 1 g of penicillin, and then the mixture was dissolved into 10 mL ultrapure water. After the aqueous solution was diluted 10 times, 10 μL of spiked penicillin solution was added into 90 μL of Au@Ag NPs colloids. The Raman spectra were directly recorded from a glass capillary tube loaded with the mixing solution using the 532-nm laser with 10 mW power and 10 × objective. The collecting time was 30 s with 5 rounds of accumulations and the pinhole aperture was 25 μm.

Accuracy of the method was determined by a standard addition technique. Known amounts of reference standard PA in a range of low, medium and high concentrations were added to preanalyzed sample of commercial penicillin and analyzed under the above measuring conditions. The experiments were replicated five times for each concentration and the accuracy was calculated as the % of analyte recovered.

2.7. Characterization and instruments

The morphologies and structures of nanoparticles were examined by a JEM-1010 transmission electron microscope (Tokyo, Japan). The hydrodynamic sizes of nanoparticles were determined using a Malvern Zetasizer Nano-ZS90 particle size analyzer (Malvern Instrument, UK). UV–vis absorption spectra were obtained by a UV-2501 spectrometer (Tokyo, Japan). Raman measurements were conducted with a Thermo Fisher DXR Raman Microscope equipped with a CCD detector in backscattered configuration using a 10 × objective (Madison, USA). The structure identification for target analyte was performed using an Agilent 6410B Triple Quad LC–ESI–MS/MS (MassHunter Data Acquisition, Qualitation and Quantitation software, USA).

3. Results and discussion

3.1. Characterizations of Au@Ag NPs

The core–shell Au@Ag NPs were prepared by seed growth through a consecutive two-step reduction process (see Supporting information) (Du et al., 2013). 30-nm Au cores were first synthesized by the chemical reduction of chloroauric acid with sodium citrate, and used as seeds for the formation of Ag nanoshells. Subsequently, silver nitrate was added into the above seed colloids and reduced with ascorbic acid under vigorous stirring, leading to

the growth of Ag nanoshells at the surface of Au seeds due to the match of crystalline lattices between Ag and Au metals. Here, the shell thickness can be controlled by the amount of silver nitrate, which can be seen by the color change of colloids from wine red to orange yellow. The transmission electron microscopic (TEM) image reveals a mondispersive particle state with an overall size of 45 ± 2.3 nm and an average shell thickness of 7 ± 0.68 nm (Fig. S1). The shell thickness was tunable from 1 to 11 nm for a fixed core of 30 nm. During the adjustment process, the plasmon resonance of the core particle was rapidly masked or attenuated by that of the growing shell, and after passing through a regime, in which two plasmon resonances were present, the shell resonance dominated. In theory, the coupling intensity is maximized when the outer metal shell has a thickness in the range of 5–10 nm (Peña-Rodríguez and Pal, 2011). When the shell thickness reached 7 nm, the resonance of Ag shell just exceeded that of Au core, which exhibited a higher Raman enhancement than monometallic Ag and Au NPs (Liu et al., 2012).

3.2. Raman enhancement mechanism

Fig. 1A shows the chemical structures of PA and penicillin. In this work, the used PA was prepared via the hydrolysis of penicillin in alkaline media and the subsequent purification (Fig. S3). Compared to penicillin, PA contains an additional carboxyl group at C_6, resulting from the opening of the β-lactam ring of penicillin. The adsorption of carboxyl groups at the surfaces of Au and Ag NPs has been well documented in many literatures (Iliescu et al., 2006; Michota and Bukowska, 2003). By the surface adsorption, the acidic carboxyl groups of citrate can play a critical role of stabilizing metal nanoparticles in colloids (Lévy et al., 2004; Tejamaya et al., 2012). However, the acidity of PA and penicillin is pKa_1 2.64 and pKa 2.75, respectively, which is obviously smaller than the pKa_1 of citrate acid (3.15). Thus, stronger acidic PA and penicillin may adsorb to the surface of Au@Ag NPs by the ligand exchange with weakly surface-bound citrate. Different from penicillin, PA molecule contains two carboxyl groups in addition to the smaller pKa_1 value. Accompanying the ligand exchange with citrate, PA will finally crosslink the Au@Ag NPs together, and the colloidal stability is drastically reduced to result in the prompt occurrence of particle aggregation (see hereinafter text). The crosslinking aggregation makes the PA molecule to be located exactly at the interspace of Au@Ag NPs for the formation of highly efficient Raman hot-spot, as shown in Fig. 1B. The PA molecule can experience a concentrated electromagnetic field at the junctions of neighboring Au@Ag NPs to obtain a huge Raman enhancement. On the contrary, penicillin molecule with one carboxyl group has less possibility to induce the particle aggregation by crosslinking to produce Raman hot-spot. The difference in Raman enhancement may provide an effective identification of trace PA residue in penicillin.

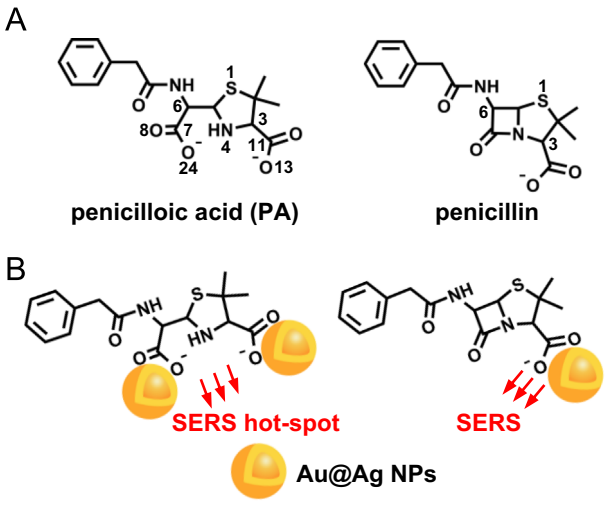

Fig. 1. (A) The chemical structures of PA and penicillin. (B) Schematic illustration for the interactions between Au@Ag NPs and PA/penicillin.

3.3. Interactions between Au@Ag NPs and PA/penicillin

Here, we first tested the interactions of Au@Ag NPs with PA and penicillin by UV–vis spectroscopy. The original Au@Ag NPs with a shell thickness of 7 nm showed a wide range of plasmon resonance absorption from 320 to 560 nm, resulting from the overlapping and coupling of two different plasmon resonance frequencies of Ag nanoshells and Au cores in the core–shell nanoparticles (the red line in Fig. 2A-a). The main peak at 395 nm was attributed to the absorption of Ag shells. Due to the coverage of Ag shells, the absorption of Au cores attenuated and appeared in a relatively weak shoulder peak in the UV–vis absorbance spectrum. With the addition of PA from 0.9 to 1.5 μM, the wide absorption significantly decreased and a new absorption at 680 nm gradually appeared and shifted toward long wavelength (Fig. 2A-a). Meanwhile, the color of Au@Ag NPs changed progressively from the original orange to grass green and finally to gray (the inset image in Fig. 2A-a), indicating that PA molecule at micro-mole levels could induce the obvious aggregation of Au@Ag NPs. Similar tests were also done on penicillin

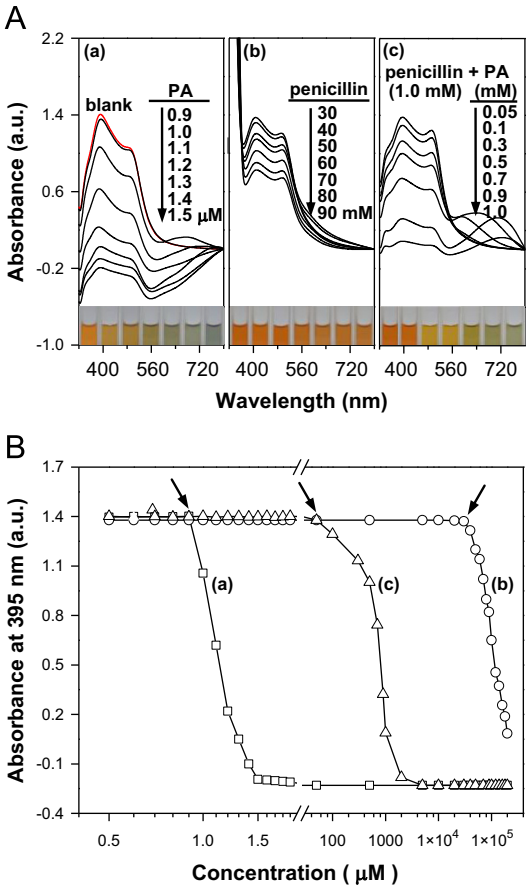

Fig. 2. (A) The UV–vis absorbance spectra of Au@Ag NPs colloids with the increase of (a) PA, (b) penicillin and (c) PA+1.0 mM penicillin (the insets show the corresponding color images). (B) The evolutions of Au@Ag NPs absorbance at 395 nm with the analyte concentrations (a, PA; b, penicillin; c, PA+1.0 mM penicillin). (For interpretation of the references to color in this figure, the reader is referred to the web version of this article.)

in Au@Ag NPs colloids (Fig. 2A-b). However, it was found that even at milli-mole levels of penicillin (30–90 mM), the absorption of Au@Ag NPs only exhibited a slight decrease and no new absorption at 680 nm was observed. In contrast to the addition of PA, the corresponding color change of Au@Ag NPs was less obvious (the inset image in Fig. 2A-b). The surprising differences on the interactions of Au@Ag NPs with PA and penicillin should be caused by the number of carboxyl groups in the two analytes. At a very low analyte concentration, PA molecule containing two carboxyl groups can link Au@Ag NPs together to result in the particle aggregation. On the contrary, the effect of particle aggregation is very weak with penicillin even at 1000 folds concentration higher than PA. The different interactions of Au@Ag NPs with PA and penicillin were also confirmed by TEM (Fig. S4) and dynamic light scattering (Fig. S5).

In order to better understand the difference of interactions, we further investigated the effect of the coexistence of penicillin and PA on the aggregation of Au@Ag NPs. Different amounts of PA were mixed into 1.0 mM penicillin aqueous solution, and then the mixing solution was added into Au@Ag NPs colloids, respectively. However, the aggregation of Au@Ag NPs occurred only when the concentration of PA was at milli-mole levels in the mixing system, as shown in the absorption spectra of Fig. 2A-c. A similar but more complex color change of Au@Ag NPs was observed in comparison with that of PA alone (the inset image in Fig. 2A-c). These observations clearly confirm that the highly concentrated penicillin in the mixing system greatly decreases the effect of particle aggregation caused by PA through the competitive adsorption of penicillin with PA at the surface of particles. From molecular structure, the carboxyl groups at C_3 of PA and penicillin have almost identical ability binding to Au@Ag NPs, which is much stronger than that at C_6 of PA due to the smaller steric hindrance. However, the single carboxyl group at C_3 has less contribution to the aggregation of particles. The above results and analysis reveal that the linking effect of two carboxyl groups in PA plays a predominant role in the aggregation of Au@Ag NPs.

Moreover, the aggregation degrees of particles induced by the two analytes were evaluated by UV–vis absorption. The strongest absorbance of Au@Ag at 395 nm was chosen as the indicator of particle-aggregating degree. As indicated by the arrow in Fig. 2B (square curve a), the critical point of Au@Ag NPs aggregation caused by PA was at ~0.9 μM. With the increase of PA content up to 1.8 μM, the aggregation of Au@Ag NPs became so severe that the nanoparticles completely precipitated. Meanwhile, the critical point of aggregation in the case of penicillin was higher up to 30 mM (Fig. 2B, the circle curve b). With the addition of mixing solution of PA and penicillin, the critical concentration of particle aggregation increased up to 0.05 mM PA (Fig. 2B, the triangle curve c), about 55 folds that of PA alone. Therefore, penicillin may stabilize the Au@Ag NPs like citrate acid, and prevent the interaction between Ag shell and PA as well as the formation of hot-spot.

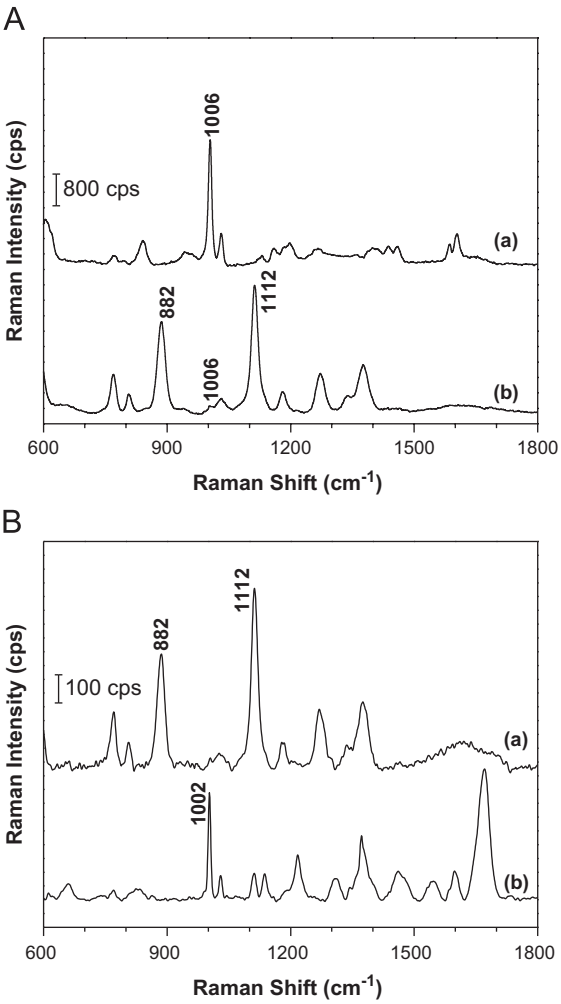

Fig. 3. (A) The Raman spectra of PA: (a) powder and (b) in Au@Ag NPs. (B) The SERS spectra of (a) PA (5×10^{-6} M) and (b) penicillin (5×10^{-2} M) in the Au@Ag NPs colloids.

3.4. SERS discrimination of PA from penicillin using Au@Ag NPs

The unique interaction of PA with Au@Ag NPs results in the spectral difference between PA powder and PA in Au@Ag NPs colloids (Fig. 3A, Table S2 and density functional theory calculations in Supporting information). In comparison with the Raman spectrum of PA powder, PA in Au@Ag NPs colloids displays two new bands at 882 and 1112 cm^{-1}, which are assigned to $\delta_s(O_{24}–C_7–O_8)$ and $\nu(C_{11}–O_{13})$ of carboxyl groups at C_6 and C_3, respectively, by density functional theory. In particular, the SERS spectrum clearly shows that the vibrational bands of two carboxyl groups are remarkably enhanced, relative to the intensity of vibration band at 1006 cm^{-1} from phenyl ring in PA powder spectrum. The selective enhancement confirms that both the carboxyl groups in PA can adsorb onto the surface of Au@Ag NPs, further leading to the formation of Raman hot-spot by cross-linking the nanoparticles.

Fig. 3B shows the SERS spectra of PA and penicillin in Au@Ag NPs colloids. The strong vibration band at 1002 cm^{-1} in penicillin is assigned to β-lactam ring (Table S3), but is not detected in PA, suggesting the opening of β-lactam ring in PA. In addition to the same band of C_3 carboxyl group at 1112 cm^{-1} for PA and penicillin, the band at 882 cm^{-1} from the carboxyl group at C_6 in PA is very strong, but does not appear in the SERS spectrum of penicillin. The difference of SERS spectroscopy provides a feasible approach to the discrimination of PA from penicillin matrix.

3.5. Raman hot-spot and Raman enhancement sensitivity

To evaluate the Raman enhancement sensitivities of Au@Ag NPs to PA and penicillin, the two analytes with a serial of concentrations were added into Au@Ag NPs colloids and the Raman spectra were recorded (Fig. S6). The Raman intensities were evaluated with the peak intensity at 1112 cm^{-1}, and the results are shown in Fig. 4. When the concentration of PA was larger than 0.08 μM, the weak Raman signal of PA could just be detected, and the intensity slowly increased with PA concentrations. However, the intensity of Raman signal greatly enhanced when the concentration exceeded 0.9 μM which was exactly the critical concentration of PA leading to the aggregation of particles (Fig. 2B-a). This suggests that the SERS of PA in Au@Ag NPs colloids

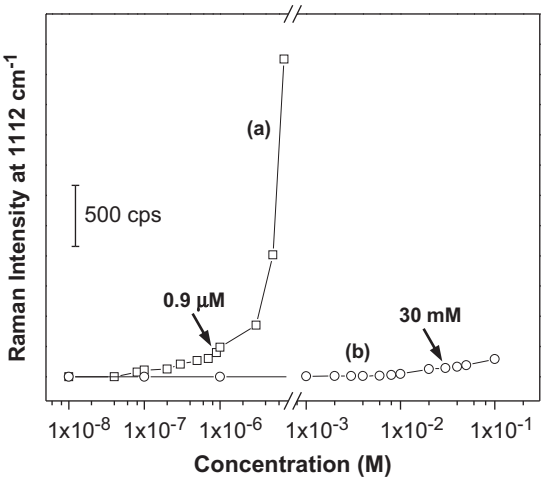

Fig. 4. The evolutions of Raman intensity at 1112 cm^{-1} with the concentrations of (a) PA and (b) penicillin.

mainly results from the contribution of Raman hot-spot. With the increase of aggregation degree, more hot-spots continuously enhanced the Raman signals of PA. In the case of penicillin, the Raman signals were still weak until the concentration reached to 0.1 M. Meanwhile, there was no sharp enhancement observed at the critical concentration of penicillin (30 mM) for the aggregation of Au@Ag NPs. That is to say, penicillin with only one carboxyl group did not produce the effective Raman hot-spot although the particle aggregation also occurred at the high concentration of penicillin. These observations are again in agreement with our expectation that the linkage of Au@Ag NPs by the two carboxyl groups of PA plays a critical role in Raman enhancement by the formation of effective hot-spot where the PA is located exactly at the interspace between Au@Ag NPs (Fig. 1B).

Moreover, the effects of Raman enhancement of Au@Ag NP on PA and penicillin can be quantitatively evaluated by SERS spectroscopy at the critical point of Au@Ag NPs aggregation. The intensity at the peak 1112 cm^{-1} can be used as the indicator of Raman enhancement. The times (F) of Raman enhancement for PA to penicillin is calculated by

$$F = \frac{I_{PA}/C_{PA}}{I_{Pen}/C_{Pen}}$$

where I_{PA} and I_{Pen} are the Raman intensities of PA and penicillin at 1112 cm^{-1}, respectively, and C_{PA} and C_{Pen} are the critical concentrations of PA (0.9 μM) and penicillin (30 mM), respectively. F is calculated to be 6.4×10^4, suggesting that the enhancement of hot-spot by Au@Ag NPs for PA is at least 4 orders of magnitude higher than that for penicillin.

3.6. Pressing effect of penicillin on SERS signals of PA

Normally, PA as a trace residue lies in penicillin matrices with a large amount, and the above results imply the inhibition of penicillin on the interaction of PA with Au@Ag NPs (Fig. 2A-c). The influence of penicillin on the SERS signals of PA has been studied by the addition of a mixing solution of PA and penicillin into Au@Ag colloids, in which the amount of PA was fixed at 100 μM and that of penicillin changed from 0 to 300 μM. Fig. 5A shows the measured Raman spectra of the mixing solutions and all peaks are attributed to PA, because the SERS signals of penicillin can only be detected at the concentration higher than 1.0 mM (Fig. S6A). With the increase of penicillin in the mixture, the SERS signals of PA significantly weakened and finally almost could not be detected at the penicillin concentration higher than 300 μM.

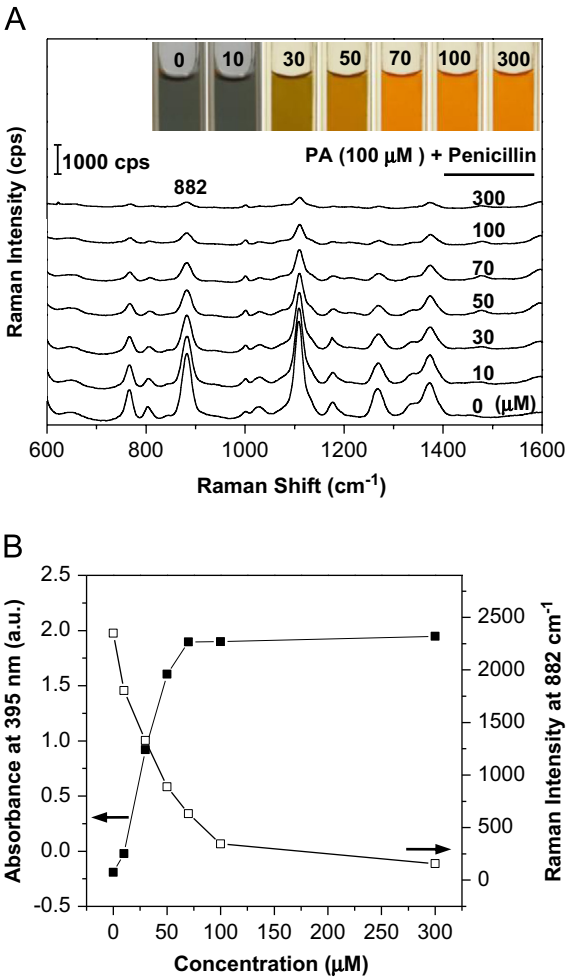

Fig. 5. (A) SERS spectra after the addition of a mixing solution of PA (a fixed 100 μM) and penicillin (changed from 0 to 300 μM) into Au@Ag colloids (the inset shows the corresponding color change). (B) Evolutions of Au@Ag NPs absorbance (at 395 nm) and PA Raman intensity (at 882 cm^{-1}) with penicillin concentrations in the mixing solution. (For interpretation of the references to color in this figure legend, the reader is referred to the web version of this article.)

On the other hand, it was noted that the increase of penicillin in the mixture obviously inhibited the Au@Ag NPs aggregation caused by PA, as shown as a colorful image in the inset of Fig. 5A. The summarized data of Au@Ag NPs absorbance and PA Raman intensity reveal that Raman intensity remarkably decreases while the absorbance becomes stronger (Fig. 5B). Two important insights into the spectroscopic behavior are confirmed here: (1) Raman hot-spot predominantly contribute to the observation of Raman signals of PA; (2) penicillin can inhibit the formation of hot-spot by the competitive adsorption with PA.

3.7. Detection of PA in penicillin

Before the detection of trace PA residue in penicillin, the detection sensitivity to individual PA analyte using the above method has been tested by the addition of 10 μL aqueous PA into Au@Ag NPs colloids. Fig. 6A shows that the Raman intensity of PA gradually increases with the concentration of PA from 1.0×10^{-7} to 5.0×10^{-6} M. The Raman intensity of the characteristic peak at 882 cm^{-1} was used for the quantitative evaluation of the PA level, plotted against the PA concentration, and exhibited a good linear relationship with the concentration ranging from 1.0×10^{-7} to

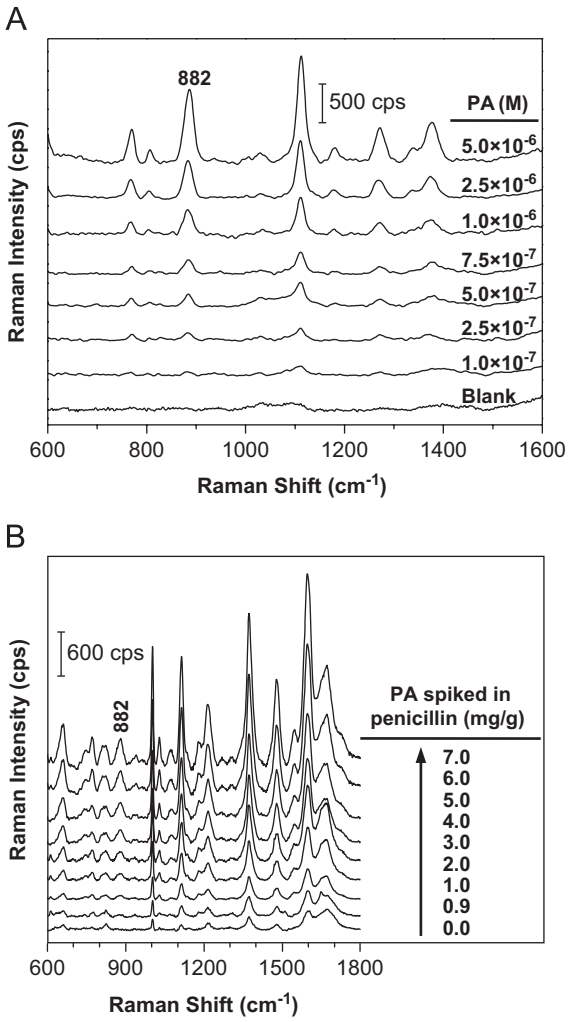

Fig. 6. (A) SERS spectra of PA in Au@Ag NPs colloids with the increase of PA amount. (B) SERS spectra of penicillin spiked with different amounts of PA in Au@Ag NPs colloids.

5.0×10^{-6} M (R^2=0.9895) (Fig. S8). The limits of detection (LOD) was determined to be 1.0×10^{-7} M (equal to 39.6 μg/L) from three standard deviations above the background.

In the detection of real sample, we spiked 0.9 to 7.0 mg PA in 1 g of penicillin, and then the aqueous solutions of the mixture were added into the Au@Ag NPs colloids. Fig. 6B shows that the specific peak of PA at 882 cm^{-1} can clearly be detected and gradually increases with the content of PA in penicillin. That is to say, the detection limit of trace PA in penicillin is down to 0.9‰ (w/w). Meanwhile, the peak intensity exhibits a good linear enhancement with PA content (Fig. S9). Thus, the method can directly detect the trace residue of PA in penicillin without any separation and purification procedure.

Furthermore, the usefulness of the SERS method was examined by the recovery of PA spiked in penicillin. Three samples were spiked with PA at the concentration of 2.0, 4.0 and 6.0 mg/g, respectively, and the data were given in Table S4. The recoveries of PA in the spiked penicillin samples were in the range of 96.23–104.77%, and the RSDs were in the range of 2.02–5.30%. The obtained data were nearly consistent with those from the liquid chromatography–mass spectrometry (LC–MS) method. All these results revealed that the SERS method could be applied to the rapid and sensitive determination of trace PA in penicillin samples.

4. Conclusions

In summary, this paper is the first report of a structure-selective hot-spot Raman enhancement method for the identification and detection of the trace PA residue in penicillin. It has been demonstrated that penicillin and PA are completely different in the interactions with Au@Ag NPs and in the enhancement effects of Raman. PA molecule with two carboxyl groups exhibits a strong linkage aggregation on Au@Ag NPs, leading to the obvious Raman hot-spot in a very low analyte concentration. In particular, the hot-spot selectively enhance the specific peak of carboxyl group formed by the opening of β-lactam ring of penicillin, and thus the spectral discrimination of PA from a large amount of penicillin can be achieved, although the penicillin has relatively strong inhibition on the formation of hot-spot. On the basis of these findings, a quantitative detection method of PA residue in penicillin has been established and meets the sensitivity requirement in real applications. In addition, the technique is very simple, inexpensive and rapid as compared to LC–MS method and each test only needs a very little amount of sample. Importantly, the rapid monitoring and tracking of allergen in penicillin may greatly reduce the possibility of occurrence of allergic reactions.

Acknowledgments

This work is supported by the National Natural Science Foundation of China (Nos. 21275075 and 21075066) and the Specialized Research Fund for the Doctoral Program of Higher Education of China (No. 20113234110001).

Appendix A. Supporting information

Supplementary data associated with this article can be found in the online version at http://dx.doi.org/10.1016/j.bios.2014.02.052.

References

Abbas, A., Brimer, A., Slocik, J.M., Tian, L.M., Naik, R.R., Singamaneni, S., 2013. Anal. Chem. 85, 3977–3983.
Batchelor, F.R., Dewdney, J.M., Gazzard, D., 1965. Nature 205, 362–364.
Batchelor, F.R., Feinberg, J.G., Dewdney, Janet M., Weston, R.D., 1967. Lancet 289, 1175–1177.
Blanca, M., Mayorga, C., Torres, M.J., Reche, M., Moya, C., Rodriguez, J.L., Romano, A., Juarez, C., 2001. Allergy 56, 862–870.
Brus, L., 2008. Acc. Chem. Res. 41, 1742–1749.
Camden, J.P., Dieringer, J.A., Zhao, J., Van Duyne, R.P., 2008a. Acc. Chem. Res. 41, 1653–1661.
Camden, J.P., Dieringer, J.A., Wang, Y., Masiello, D.J., Marks, L.D., Schatz, G.C., Van Duyne, R.P., 2008b. J. Am. Chem. Soc. 130, 12616–12617.
Degelaen, J.P., Loukas, S.L., Feeney, J., Roberts, G.C., Burgen, A.S., 1979. J. Chem. Soc., Perkin Trans. 2, 86–90.
Du, Y.X., Liu, R.Y., Liu, B.H., Wang, S.H., Han, M.Y., Zhang, Z.P., 2013. Anal. Chem. 85, 3160–3165.
Ghebre-Sellassie, I., Hem, S.L., Knevel, A.M., 1984. J. Pharm. Sci. 73, 125–128.
Iliescu, T., Baia, M., Pavel, I., 2006. J. Raman Spectrosc. 37, 318–325.
Jeanmaire, D.L., Van Duyne, R.P., 1977. J. Electroanal. Chem. 84, 1–20.
Levine, B.B., Ovary, Z., 1961. J. Exp. Med. 144, 875–904.
Lévy, R., Thanh, N.T., Doty, R.C., Hussain, I., Nichols, R.J., Schiffrin, D.J., Brust, M., Fernig, D.G., 2004. J. Am. Chem. Soc. 126, 10076–10084.
Li, D., Yang, M., Hu, J., Zhang, Y., Chang, H., Jin, F., 2008. Water Res. 42, 307–317.
Li, Y.T., Qu, L.L., Li, D.W., Song, Q.X., Fathi, F., Long, Y.T., 2013. Biosens. Bioelectron. 43, 94–100.
Liu, B.H., Han, G.M., Zhang, Z.P., Liu, R.Y., Jiang, C.L., Wang, S.H., Han, M.Y., 2012. Anal. Chem. 84, 255–261.
Mendelson, L.M., Ressler, C., Rosen, J.P., Selcow, J.E., 1984. J. Allergy Clin. Immunol. 73, 76–81.
Michota, A., Bukowska, J., 2003. J. Raman Spectrosc. 34, 21–25.
Nie, S., Emory, S.R., 1997. Science 275, 1102–1106.
Pan, S.C., 1954. Anal. Chem. 26, 1438–1444.
Peña-Rodríguez, O., Pal, U., 2011. Nanoscale Res. Lett. 6, 279–283.
Pieczonka, N.P.W., Aroca, R.F., 2008. Chem. Soc. Rev. 37, 946–954.
Pichichero, M.E., 2005. Pediatrics 115, 1048–1057.

Qian, X.M., Nie, S.M., 2008. Chem. Soc. Rev. 37, 912–920.
Smith, H., Marshall, A.C., 1971. Nature 232, 45–46.
Smith, W.E., 2008. Chem. Soc. Rev. 37, 955–964.
Sogn, D.D., 1984. J. Allergy Clin. Immunol. 74, 589–593.
Tejamaya, M., Römer, I., Merrifield, R.C., Lead, J.R., 2012. Environ. Sci. Technol. 46, 7011–7017.
Torres, M.J., Mayorga, C., Pamies, R., Juarez, C., Blanca, M., Romano, A., 1999. Allergy 54, 936–943.
Weltzien, H.U., Padovan, E., 1998. J. Invest. Dermatol. 110, 203–206.
Wu, L., Wang, Z.Y., Zong, S.F., Huang, Z., Zhang, P.Y., Cui, Y.P., 2012. Biosens. Bioelectron. 38, 94–99.
Zhang, Y., Jiang, Y., Wang, S., 2010. J. Agric. Food Chem. 58, 8171–8175.